V.A. Romaka[1,2], P. Rogl[3], V.V. Romaka[2], Yu.V. Stadnyk[4], R.O. Korzh[2], A.M. Horyn[4], V.Ya. Krajovsky[2], O.I. Lakh[5]

[1]Ya. Pidstryhach Institute for Applied Problems of Mechanics
and Mathematics National Academy of Sciences of Ukraine,
3-b, Naukova Str., Lviv, 79060, Ukraine;
[2]National University "Lvivska Polytechnika", 12, S.Bandera Str., Lviv, 79013,Ukraine;
[3]Ivan Franko National University of Lviv, 6, Kyryla and Mefodiya Str., Lviv, 79005, Ukraine;
[4]Institut für Physikalische Chemie, Universität Wien, 42, Währinger Str.,
Wien, A-1090, Österreich;
[5]Closed JSC V.I. Lakh "NVO "Thermoprylad", 3, Naukova Str., Lviv, 79060, Ukraine

OPTIMIZATION OF PARAMETERS OF THE NEW THERMOELECTRIC MATERIAL $HfNiSn_{1-x}Sb_x$

The crystalline and electronic structures, temperature and concentration dependences of resistivity and the Seebeck coefficient of n-HfNiSn intermetallic semiconductor doped with Sb were investigated in the temperature range $T = 80 \div 400$ K. The main mechanisms of conduction were established and they are in agreement with the results of theoretical studies of electronic structure of $HfNiSn_{1-x}Sb_x$. It was predicted and shown that the obtained thermometric material $HfNiSn_{1-x}Sb_x$ has high efficiency of thermal into electrical energy conversion.
Key words: electronic structure, Fermi level, resistivity, Seebeck coefficient.

Introduction

Intermetallic semiconductor *n-HfNiSn* is known to possess high efficiency of thermal into electric energy conversion, though insufficient for industrial application [1]. At the same time, optimization of parameters of thermoelectric materials to obtain maximum values of thermoelectric figure of merit depends on a number of factors, in particular, current carrier concentration, scattering mechanisms, thermal conductivity, the choice of crystallographic orientation, etc. One of the methods for improving the thermoelectric figure of merit of semiconductor materials is their doping [1, 2].

In [3] it was shown that in the intermetallic semiconductors of *MgAgAs* structural type (half-Heusler alloys) a pre-requisite for achieving maximum efficiency of thermal into electric energy conversion is semiconductor doping with such type of impurities that would coincide with the type of major carriers of base semiconductor matrix.

On the other hand, investigations [4] showed that crystalline structure of *HfNiSn* compound is disordered, namely position of *Hf* ($5d^26s^2$) atoms up to ~ 1 % is occupied with *Ni* ($3d^84s^2$) atoms, which generates donor defects in crystal structure. Exactly this structural feature of *HfNiSn* accounts for the mechanism of "a priori doping" the semiconductor with a donor impurity.

Thus, in conformity with conclusions of [3], to improve the efficiency of thermal into electric energy conversion, the semiconductor *n-HfNiSn* must be doped with such type of impurity which would generate donor-nature defects in the crystal. One of the variants of such doping is introduction into *HfNiSn* compound of *Sb* ($4d^{10}5s^25p^3$) atoms through substitution of *Sn* ($4d^{10}5s^25p^2$) atoms. As long

as *Sb* atom has one 5*p*-electron more than *Sn* atom, such substitution should have generated donor-nature structural defects in the crystal. In this case, on should expect increase in the efficiency of thermal into electric energy conversion in $HfNiSn_{1-x}Sb_x$ when the Fermi level approaches the level of semiconductor conduction band.

The purpose of this paper is to study the prospects of using the new thermoelectric material $HfNiSn_{1-x}Sb_x$ for thermal into electric energy conversion. The proposed complex work studies the mechanism and conditions for entry of *Sb* atoms into the structure of *HfNiSn* compound with employment of experimental analysis methods, as well as calculations of its electronic structure. In particular, the dynamics of change in crystalline structure of $HfNiSn_{1-x}Sb_x$ will be investigated, the region of solid solution existence will be established, as well as simulation of electronic structure and thermodynamic calculations will be performed. Besides, the electrokinetic and energy characteristics of $HfNiSn_{1-x}Sb_x$ will be analyzed, as well as the experimental and calculated results will be compared, wherefrom will follow the degree of adequacy of the proposed models of crystalline and electronic structures of semiconductor.

Investigation methods

The object to be investigated included crystalline structure, electron density distribution (DOS), electrokinetic and energy characteristics of $HfNiSn_{1-x}Sb_x$. The samples were synthesized in the laboratory of Institute for Physical Chemistry, Vienna University. The *X*-ray structural analysis [5] with employment of Fullprof program [6] was used to obtain the values of $HfNiSn_{1-x}Sb_x$ crystal lattice periods. The data arrays obtained by powder method were used (diffractometer Guinier-Huber image plate system, $CuKa_1$-radiatione; $8° \leq 2\theta \leq 100°$). The chemical and phase compositions of samples were controlled by scanning electron microscope (SEM, Zeiss Supra 55VP) and microprobe analyzer (EPMA, energy-dispersive *X*-ray analyzer). The electronic structure calculations were performed by the Korringa-Kohn-Rostoker (KKR) methods in coherent potential approximation (CPA), local density approximation (LDA) and plane wave approximation (FP-LAPW) in the framework of density functional theory (DFT) [7]. The temperature and concentration dependences of the electrical resistivity ρ and the Seebeck coefficient α of $HfNiSn_{1-x}Sb_x$ were measured in the ranges: $T = 80 \div 400$ K, $N_D^{Sb} \approx 9.5 \cdot 10^{19}$ cm^{-3} ($x = 0.005$) $\div$ $1.9 \cdot 10^{21}$ cm^{-3} ($x = 0.10$).

Research on structural features of $HfNiSn_{1-x}Sb_x$

To verify the above stated assumption as to the method of doping *n-HfNiSn* for obtaining the new thermoelectric material with high thermoelectric power values, samples were synthesized where *Sn* atoms were substituted by *Sb* atoms. The microprobe analysis of the concentration of atoms on the surface and cleavages of $HfNiSn_{1-x}Sb_x$ samples has showed their conformity to the initial charge compositions, which is one of the experimental proofs of predicted substitution of *Sn* atoms by *Sb* atoms. In their turn, the *X*-ray phase and structural analyses have shown that all the investigated samples of $HfNiSn_{1-x}Sb_x$ have no traces of other phases, except for the basic one, up to the composition $x = 0.1$ inclusive (structural type *MgAgAs*, cubic syngony, space group $F\bar{4}3m$). According to *X*-ray phase analysis, the synthesized samples of solid solution $HfNiSn_{1-x}Sb_x$ are single-phase up to $x = 0.1$ inclusive. Research on the structure of $HfNiSn_{1-x}Sb_x$ detected the substitution of *Sn* atoms by *Sb* atoms, leading to a regular growth of unit cell period $a(x)$ (Fig. 1 *a*). These results agree with the difference in atomic radii of *Sn* ($r_{Sn} = 0.158$ nm) and *Sb* ($r_{Sn} = 0.160$ nm).

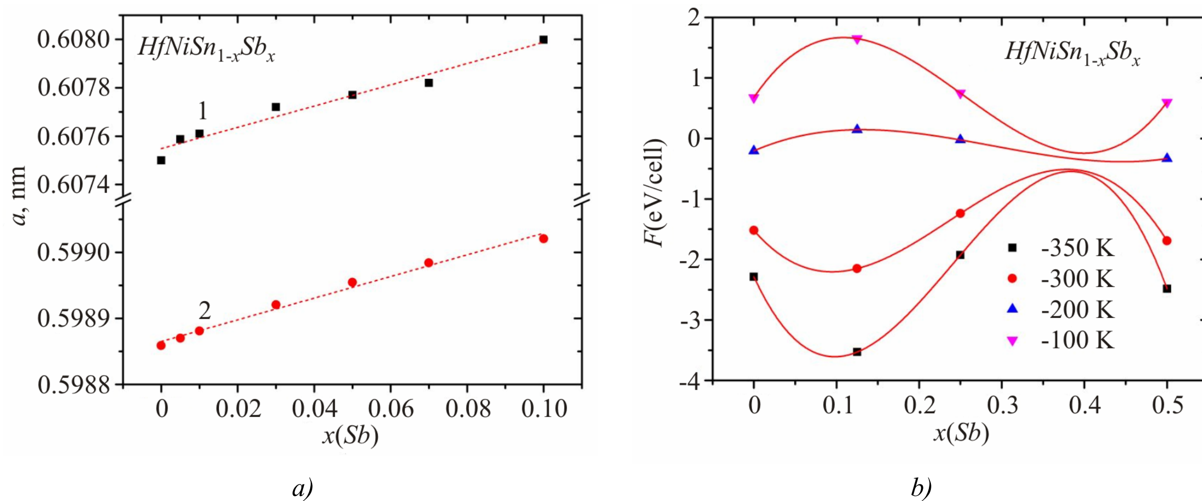

Fig. 1. a) Change in a(x) period values: 1 – experimental value; 2 – calculated values; b) free energy F(x) of $HfNiSn_{1-x}Sb_x$.

The refinement of crystalline structure by powder method has shown that the degree of occupancy of atomic position *Sn*(*Sb*) is 100 %, and the structure of $HfNiSn_{1-x}Sb_x$ is ordered, which creates prerequisites for obtaining semiconductor material with unambiguous characteristics that do not change during many cycles of samples heating and cooling. Note that the ordering of $HfNiSn_{1-x}Sb_x$ structure means that with the lowest concentrations of *Sb* atoms which occupy the position of *Sn* atoms, there is a parallel process of return of 1 % of *Ni* atoms that occupied the crystallographic position of *Hf* to their own crystallographic position [4].

Optimization of the values of unit cell period $a(x)$ of $HfNiSn_{1-x}Sb_x$ for the concentrations $x(Sb) = 0$, 0.25 and 0.5 yielded its concentration dependence (Fig. 1 *a*). Calculations confirmed growth of unit cell parameter, but with a positive deviation from linearity. As long as the use of local density approximation leads to underestimation of the values of energy and unit cell periods, the resulting calculated values of unit cell period $a(x)$ (Fig. 1 *a*) are systematically underrated with respect to experimental values, but the tendency remains practically the same.

In their turn, thermodynamic calculations with the use of DFT in the approximation of harmonic fluctuations of atoms have shown that dependence of free energy (Helmholtz potential) at a temperature of 350 K passes through the minimum (Fig. 1 *b*) at concentration $x(Sb) \approx 0.1$, thus indicating the restricted solubility of *Sb* atoms in crystalline structure of *HfNiSn*, which is experimentally confirmed, but differs essentially from the solubility of rare-earth metal atoms in *HfNiSn* which makes ~ 0.3 [1]. Moreover, from Fig. 1 *b* it follows that with a rise in temperature the solubility of *Sb* atoms in *HfNiSn* structure is increased.

On the other hand, calculations of the distribution of electron localization function (ELF) in the initial *HfNiSn* and doped $HfNiSn_{1-x}Sb_x$ compounds point to additional electron density localization between *Ni* and *Sb* atoms (Fig. 2), which is indicative of electron density growth in crystal due to donor impurity nature. Based on this result it can be concluded that the substitution of *p*-element in crystal structure of *HfNiSn* produces a much larger effect on its stability than the substitution of *Hf* or *Ni* atoms. This is because a system of tetrahedral ion-covalent bonds is formed due to tetrahedral hybridization of *Sn* atomic orbitals, and any essential changes in the number of valence electrons on *p*-orbitals will result in formation of more energetically beneficial chemical bonds and, as a consequence, in the destruction of *MgAgAs* type structure [4, 8].

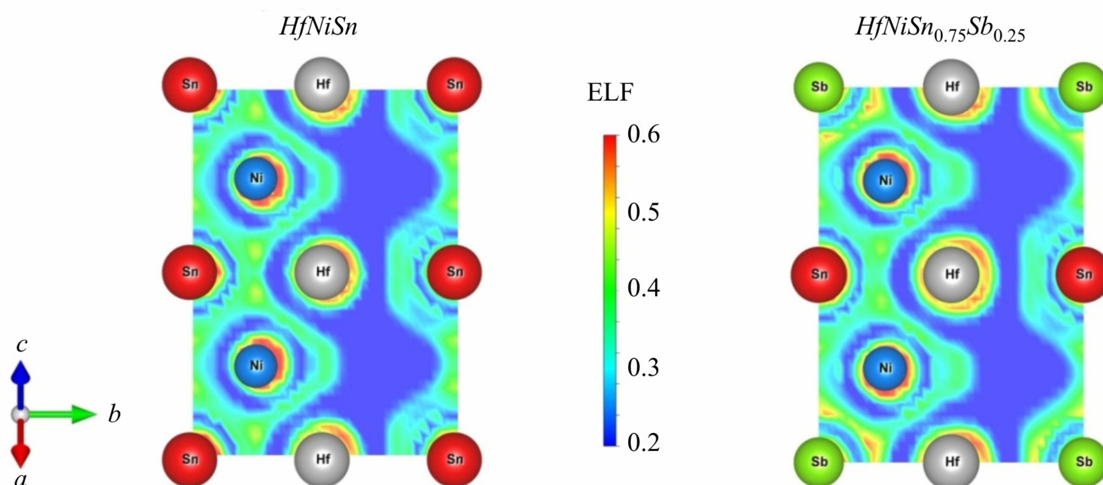

Fig. 2. Projection of electron localization function (ELF) on the plane [101] for the initial compound HfNiSn and for compound $HfNiSn_{0.75}Sb_{0.25}$.

Therefore, structural investigations of *n-HfNiSn* doped with *Sb* atoms have demonstrated that S*b* atoms occupy exceptionally crystallographic position of *Sn* atoms, generating donor-nature structural defects in the crystal, and the solubility area of *Sb* atoms in $HfNiSn_{1-x}Sb_x$ matrix is $x \leq 0.10$.

Research on the electron structure of $HfNiSn_{1-x}Sb_x$

To predict the behaviour of the Fermi level ε_F, the energy gap ε_g and the electrokinetic characteristics of *n-HfNiSn* doped with *Sb* atoms, the electron density distribution (DOS) of $HfNiSn_{1-x}Sb_x$ was calculated. In view of the fact that introduction into *HfNiSn* compound of impurity *Sb* atoms puts in order its crystalline structure, calculations of DOS were performed for the case of ordered crystalline structure.

As indicated above, introduction of *Sb* atoms into crystalline structure of *HfNiSn* compound is accompanied by generation of donor-nature structural defects. In this case, doping with donor impurities the intermetallic semiconductor *n-HfNiSn* the structure of which already has donor defects will reduce the compensation degree, and the Fermi level will drift in the direction of conduction band that will be crossed at certain concentrations of *Sb* impurity atoms. Fig. 3 *a* shows the results of calculation of electron density distribution, variation in energy gap and the Fermi level position for the ordered variant of $HfNiSn_{1-x}Sb_x$ crystalline structure. It is obvious that on introducing into *n-HfNiSn* the least attainable in the experiment concentrations of *Sb* donor impurity, the Fermi level ε_F moves from the energy gap where in *n-HfNiSn* it was located near the bottom of conduction band at the distance of ~ 81.3 meV [9] to conduction band, i.e. dielectric-metal transition is realized, which is Anderson transition [10]. With increase in donor impurity concentration, the Fermi level drifts in the band of continuous energies. Apart from the drift caused by a reduction in semiconductor compensation degree, there is also a reduction in the values of semiconductor effective energy gap ε_g from ε_g ($x = 0$) = 287.7 meV to ε_g ($x = 0.01$) = 181.7 meV due to increase of band "tails" changing the profile of continuous energy bands (Fig. 3 *a*).

Such Fermi level behaviour caused by ordering semiconductor crystalline structure allows predicting the conductivity mechanisms and electrokinetic characteristics of semiconductor solid solution $HfNiSn_{1-x}Sb_x$. Having calculated the electron structure of $HfNiSn_{1-x}Sb_x$, one can predict the

behaviour of its electrokinetic characteristics, and Fig. 3 *b*, as a reference, shows a change in the Seebeck coefficient values of $HfNiSn_{1-x}Sb_x$ at different temperatures.

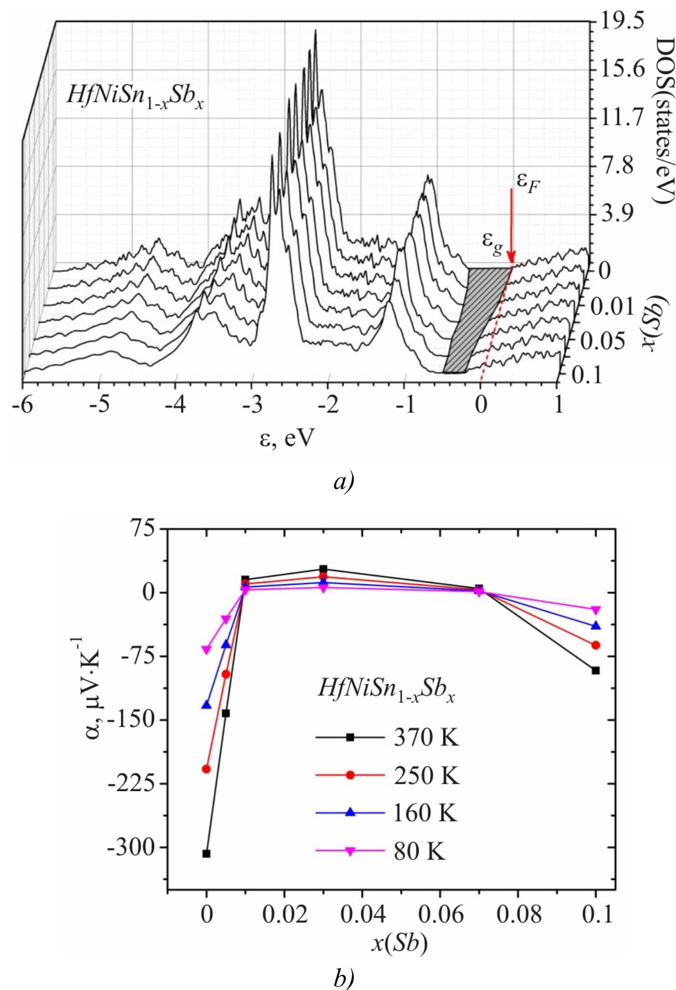

Fig. 3. Electron density distribution DOS (a) and calculations of variation in the values of the Seebeck coefficient α(x) at different temperatures (b) of $HfNiSn_{1-x}Sb_x$.

A low concentration of impurities whereby there is dielectric-metal transition allows purposeful getting in $HfNiSn_{1-x}Sb_x$ high values of the Seebeck coefficient α and electric conductivity σ, which will assure high values of thermoelectric power factor $Z^* = \alpha^2/\sigma$. Moreover, high values of the Seebeck coefficient α of $HfNiSn_{1-x}Sb_x$ in a wide temperature range make this solid solution also a promising thermometric material for the manufacture of sensitive elements of thermoelectric thermometers.

Thus, the results of calculations of electron density distribution of $HfNiSn_{1-x}Sb_x$ based on the results of structural investigations point to the donor nature of generated structural defects, and the experimental investigations will test the adequacy of calculated results, hence of selected model of semiconductor structure.

Research on the electrokinetic and energy characteristics of $HfNiSn_{1-x}Sb_x$

Fig. 4 presents the temperature dependences of electric resistivity ρ and the Seebeck coefficient $\alpha(1/T)$ for samples of $HfNiSn_{1-x}Sb_x$, $0 \le x \le 0.10$ which vary in full conformity with the results of calculations of electron density distribution.

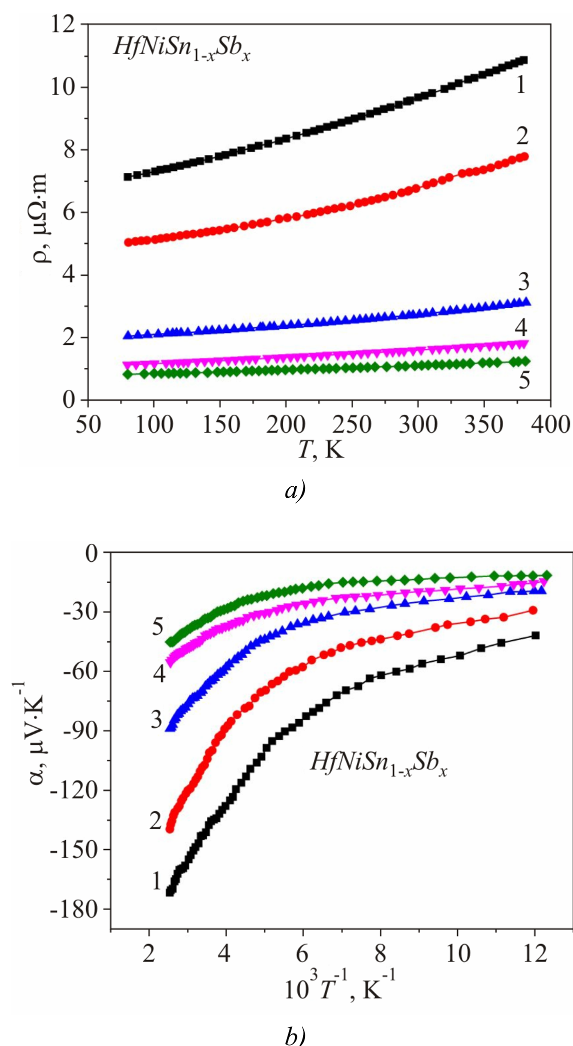

Fig. 4. Temperature dependences of electric resistivity ρ *(a) and the Seebeck coefficient* α *(b) of $HfNiSn_{1-x}Sb_x$: 1 – x = 0.005; 2 – x = 0.01; 3 – x = 0.03; 4 – x = 0.07; 5 – x = 0.10.*

Adding the lowest concentration of *Sb* atoms leads to increase in the values of electric resistivity (ρ) with a rise in temperature and the absence of activation areas on its temperature dependences. Such behaviour of $\rho(T)$ is typical of metallic conductivity type, which is possible when the Fermi level ε_F approaches the edge of conductivity band by the value close to k_BT, or in the case of entry into the zone of continuous energies.

Moreover, the electric resistivity values drastically decrease (Fig. 5 *a*) with increase in the concentration of *Sb* impurity atoms in the structure of *HfNiSn* compound, which is possible only with generation in crystal of donor-nature defects and increase in the concentration of free electrons. Thus, for instance, at $T = 80$ K the value of $\rho(x)$ drastically decreases from $\rho_{x=0} = 1071.1$ μΩ·m to the value of $\rho_{x=0.005} = 7.14$ μΩ·m. Such behaviour of $\rho(x)$ is caused by increase in the values of density of states on the Fermi level with a decrease in semiconductor compensation degree, which was anticipated by the calculations of its electronic structure. The fact that the Fermi level is displaced exactly in the direction of conduction band on doping *n-HfNiSn* with *Sb* donor impurity is shown by the dependences of variation in the Seebeck coefficient values over the entire temperature and concentration ranges (Fig. 5 *b*). Thus, the value of the Seebeck coefficient, for instance, at 80 K, varies

from $\alpha_{x=0} = -178.1$ μVK^{-1} to the value of $\alpha_{x=0.005} = -41.5$ μVK^{-1}, which points to approaching by the Fermi level the edge of semiconductor conduction band.

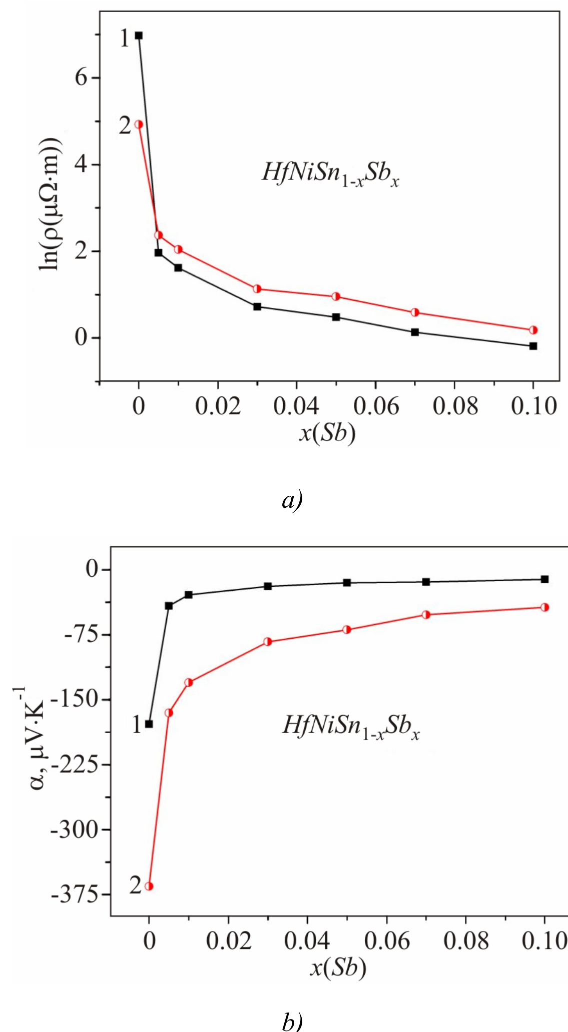

Fig. 5. Change in the values of electric resistivity ρ(x) (a) and the Seebeck coefficient α(x) (b) of $HfNiSn_{1-x}Sb_x$ at different temperatures: 1 – T = 80 K; 2 – T = 380 K.

One of the arguments that *Sb* impurity atoms generate donor defects in the structure of *HfNiSn* compound is the character of variation in the amplitude of large-scale fluctuation of continuous-energy bands (ε_1^{α}) and the averaged amplitude of potential well of small-scale fluctuation (ε_3^{α}) (Fig. 6 *a*) of $HfNiSn_{1-x}Sb_x$, calculated by the high- and low-temperature areas of $\alpha(1/T)$ dependences, respectively [1].

Introduction into *n-HfNiSn* of *Sb* donor impurity is accompanied by a reduction in semiconductor compensation degree [10], which will cause a reduction in the values of fluctuation amplitude (a reduction in the values of ε_1^{α}). Moreover, there is also a correlation between the amplitude values of large-scale fluctuation ε_1^{α} and the potential well depth of small-scale fluctuation ε_3^{α}, namely the lower the fluctuation amplitude, the smaller the potential well of small-scale fluctuation [10].

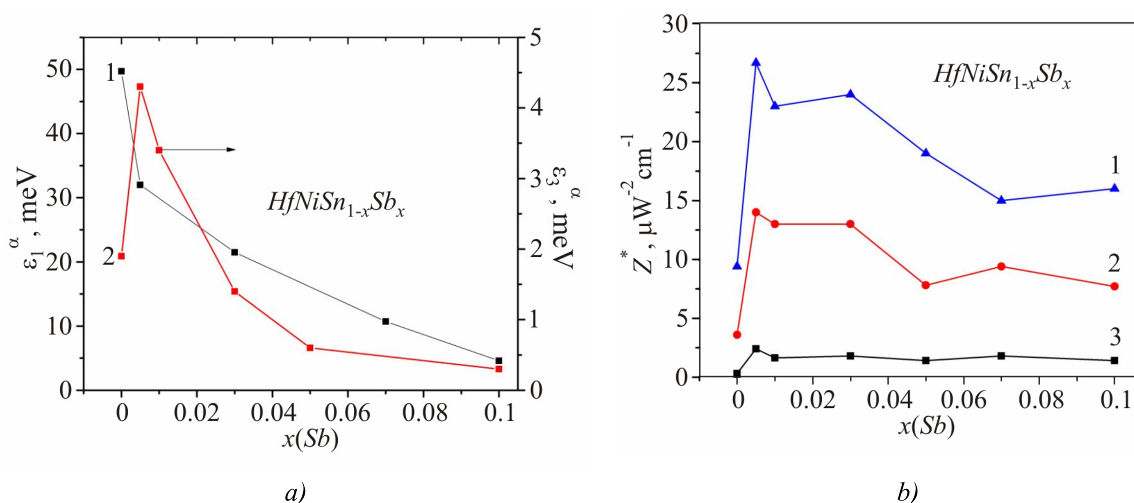

Fig. 6. Change in the values of activation energies ε_1^α (1) and ε_3^α (2) (a) and thermoelectric power factor Z (b) of $HfNiSn_{1-x}Sb_x$ at different temperatures: 1 – T = 380 K; 2 – T = 250 K; 3 – T = 80 K.

Thus, doping of intermetallic semiconductor *n-HfNiSn* with *Sb* donor impurity is characterized by increase in electric conductivity values with relatively high values of thermopower factor. This is a guarantee of obtaining high values of thermoelectric power factor in a semiconductor solid solution $HfNiSn_{1-x}Sb_x$.

Research on thermoelectric power factor of $HfNiSn_{1-x}Sb_x$

Fig. 6 *b* represents the concentration dependences of change in thermoelectric power factor Z^* of $HfNiSn_{1-x}Sb_x$. We can see that exactly at the lowest concentration of donor impurity, $x = 0.005$, the values of thermoelectric power factor are maximum. Such a behaviour of $Z^*(x)$ of $HfNiSn_{1-x}Sb_x$ is understandable and was expected on the basis of calculations of semiconductor electron density distribution.

Conclusions

Thus, based on the foregoing results we can assert that the obtained solid solution $HfNiSn_{1-x}Sb_x$ is a new promising thermoelectric material, and in its characteristics, in particular, the values of thermoelectric power factor, it outperforms considerably *n-HfNiSn*. Moreover, the values of thermoelectric power factor increase with a rise in temperature, which expands the range of their possible application.

The work was performed in the framework of grant of the National Academy of Sciences, № 106U000594.

References

1. V.A. Romaka, V.V. Romaka, and Yu.V. Stadnyk, *Intermetallic Semiconductors: Properties and Applications* (Lviv, Lvivska Polytechnika, 2011), 488 p.
2. L.I. Anatychuk, *Thermoelements and Thermoelectric Devices* (Kyiv: Naukova Dumka, 1979), 768 p.
3. V.A. Romaka, D. Fruchart, Yu.V. Stadnyk, J. Tobola, Yu.K. Horelenko, M.G. Shelyapina, L.P. Romaka and V.F. Chekurin, Conditions for the Attainment of Maximum Values of Thermo-

electric Power Factor in the Intermetallic Semiconductors of *MgAgAs* Structural Type, *Semiconductors* **40** (11), 1289 – 1395 (2006).
4. V.V. Romaka, P. Rogl, L. Romaka, Yu. Stadnyk, A. Grytsiv, O. Lakh, and V. Krajovsky, Peculiarites of Structural Disorder in *Zr*- and *Hf*-Containing Heusler and Half-Heusler Stannides, *Intermetallics* **35**, 45 – 52 (2013).
5. V.K. Pecharsky, P.U. Zavalij, *Fundamentals of Powder Diffraction and Structural Characterization of Materials* (NY, Springer, 2005), 713 p.
6. T. Roisnel, J. Rodriguez-Carvajal, WinPLOTR: a Windows Tool for Powder Diffraction Patterns Analysis, *Mater. Sci. Forum, Proc. EPDIC7* **378** – **381**, 118 – 123 (2001).
7. M. Schröter, H. Ebert, H. Akai, P. Entel, E. Hoffmann and G.G. Reddy, First-Principles Investigations of Atomic Disorder Effects on Magnetic and Structural Instabilities in Transition-Metal Alloys, *Phys. Rev. B* **52**, 188 (1995).
8. V.K. Grigorovich, *Metallic Bond and Structure of Metals* (Moscow: Nauka, 1988), 296 p.
9. V.A. Romaka, P. Rogl, V.V. Romaka, Yu.V. Stadnyk, E.K. Hlil, V.Ya. Krajovsky, and A.M. Horyn, Features of Conduction Mechanisms in *n-HfNiSn* Semiconductor Heavily Doped with *Rh* Acceptor Impurity, *Semiconductors* **47** (9), 1145 – 1152 (2013).
10. B.I. Shklovsky, A.L. Efros, *Electronic Properties of Doped Semiconductors* (Moscow: Nauka, 1979), 416 p.

Submitted 06.11.2013.